AVENTICS

Proceedings of 2nd Agria Conference on Innovative Pneumatic Vehicles – ACIPV 2018

May 11, 2018 Eger, Hungary

AVENTICS Pneumobil

Proceedings

of the

2nd Agria Conference on Innovative Pneumatic Vehicles ACIPV 2018

May 11, 2018
Eger, Hungary

Edited by
Prof.Dr. László Pokorádi

Published by
Óbuda University, Institute of Mechatronics and Vehicle Engineering

ISBN 978-963-449-089-0

Technical Sponsor:

Aventics Hungary Kft.

Organizer:

Óbuda University, Institute of Mechatronics and Vehicle Engineering

Honorary Chairs:

László Palkovics, BUTE, Budapest
Mihály Réger, Óbuda University, Budapest

Honorary Committee:

István Gödri, Aventics Hungary Kft., Eger
Zoltán Rajnai, Óbuda University, Budapest

General Chair:

László Pokorádi, Óbuda University, Budapest

Scientific Program Committee Chair:

József Zoltán Szabó, Óbuda University, Budapest

Scientific Program Committee:

János Bihari, University of Miskolc
Zsolt Farkas, Budapest University of Technology and Economics
Lucian Fechete, Technical University of Cluj-Napoca
Wieslaw Fiebig, Wroclaw University of Science and Technology
Dénes Fodor, University of Pannonia
Zoltán Forgó, Sapientia Hungarian University of Transylvania
György Juhász, University of Debrecen
Gábor Kátai-Urbán, Neumann János Egyetem
László Kelemen, University of Miskolc
Tomáš Kroutil, Brno University of Technology
János Líska, Neumann János Egyetem
Marten Madissoo, Estonian University of Life Sciences
Ghinea Mihai, University POLITEHNICA of Bucharest
Vilnis Pirs, Latvian University of Agriculture
Krzysztof Psiuk, Silesian University of Technology
Mihai Simon, Universitatea Petru Maior
István Péter Szabó, Szegedi Tudományegyetem
Janis Rudzitis, Riga Technical University
Tibor Szabó, Budapest University of Technology and Economics
Pawel Sliwinski, Gdańsk University of Technology
Tibor István Tóth, University of Szeged
Tibor Vesselenyi, University of Oradea

Organizing Committee Chair:

Endre Tamás, *Aventics Hungary Kft., Eger*

Organizing Committee:

Enikő Pekk, *Aventics Kft., Eger*
Ferenc Bolyki, *Aventics Kft., Eger*

CONTENTS

2nd Agria Conference
on Innovative Pneumatic Vehicles
ACIPV 2018
program

09:00 – 09:10	Welcome speech *István Gödri*	Room KÖRIS
PLENARY SECTION chairman: *László Pokorádi*		
09:10 – 09:30	*Wolf Gerecke* Industrial Internet of Things as a Driver for Smart Pneumatic Components	
09:30 – 09:50	*Botond Barabás* Industrial Internet of Things at NI Hungary Kft.	
09:50 – 10:10	*Marten Madissoo, Kristjan Türk* Optimized Valve System for a Pneumatic Motor	
coffee break		
SECTION chairman: *József Zoltán Szabó*		Room KÖRIS
10:30 – 10:50	*Zoltán Márton. Dénes Fodor.* Adaptive control based air expansion range extension of pneumatic vehicles	
10:50 – 11:10	*Bence Márk Szeszák, György Juhász, Gusztáv Áron Sziki, Rita Nagy-Kondor, Tamás Sádor Sütő* Analysis of the Rolling Resistance of Pneumobils for Vehicle Dynamics Modelling Purpose	
11:10 – 11:30	*János Bihari, Ferenc Sarka* Human-electric hybrids and reaching times in commuting	
11:30 – 11:50	*Tamás Szakács* Pneumatic modelling of a pneumobil	
11:50 – 11:55	Closing speech *László Pokorádi*	

Disclaimer

Copyright

Optimized Valve System for a Pneumatic Motor

M. Madissoo *, K. Türk *

** Estonian University of Life Sciences, Institute of Technology, Fr.R.Kreutzwaldi 56/1, Tartu 51014 Estonia (Tel: +372 55617070; e-mail: marten.madissoo@emu.ee).*

Abstract: The aim of this article is to give an overview of the development and construction of a pneumatic valve system with improved features. The properties of the developed valve are compared to the Aventics valve CD12. Compared to the standard valve the developed valve system has, higher capacity, less weight and lower pressure drop through the valve at the same flow rate. The analysis of the CD12 valve was performed using CFD method. Based on the analysis, a prototype valve was designed in a configuration that allowed the testing of its parameters. The performed tests and analyzes showed that the new valve system design was justified. The tests also unveiled some weaknesses of the new valve which were identified and solved. Subsequently, a 2x2/2 valve was designed and constructed. The valve was analyzed again by the CFD method and it was concluded that the valve has a significantly higher flow rate and greater efficiency, at an equivalent flow, than the compared CD12 valve. The design, analyze and operation performance details of the valve system will be described extensively in the Article.

1. INTRODUCTION

In the case of pneumatic systems, efficiency is very important as the production of compressed air is very costly, due to the low efficiency of the compressors, pressure losses and leakage in the system. As for the compressed air vehicles designed under the Pneumobile project, it is important to always find solutions to optimize the system components for gaining an advantage at the competition. It also allows you to use solutions that are not considered by the industry, but by demonstrating their function and utility they also can help to improve industry-specific systems. Because of that it was decided to design a new optimised valve system.

In this work, the pneumatic chain of the latest compressed air vehicle “Technics 4” is optimized for the Pneumatic 2018 project. To achieve high efficiency, the complexity and resistance, the system was analysed with the CFD method. CFD, or Computational Flow Dynamics (J. F. Wendt 1995), is a finite element method that allows analyzing fluid and gas flow processes. The method allows quantifying the effect of structural elements on the valve throughput, and gives an overview of the flow characteristics due to the geometry of the subject being studied. That's why it's possible to optimize the valve design. In order to evaluate the analysis, a standard Aventics CD12 valve is used as a benchmark of which the parameters are known and specified by the manufacturer. In this way, it is possible to compare the proxies of the analyzes made by the given software with actual results obtained in real life.

The measurable results which were compared were capacity and pressure drop through the valve at the same flow rate.

2. MATERIALS AND METHODS

The standardized method evaluates the flow coefficient using the valve throughput. The flow coefficient allows you to evaluate the valve's resistance taking into account pressure drop, gas temperature and flow (M. S. James 2002). This coefficient is determined on an experimental path, the test scheme of which is given in Fig 1.

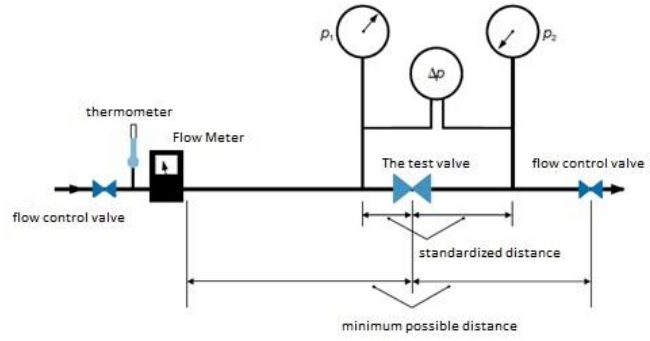

Fig. 1. Schematic for determining the flow coefficient (Swagelok 2018)

The calculations and test settings are in accordance with the standard for determining the flow characteristics for the available standards ANSI / ISA-S75.02-1996 and ISA-75.01.01-2007 (ISA1996, 2007). The standards indicate that the tests must be performed in maximum flow mode. With a flow meter recommended flow of 4000 L/min. Purchase of such a sensor is out of our project budget so it is decided to find alternative ways to perform flow analysis.

To assess the capability of the valves, a number of parametric controlled simulations are performed to determine the characteristic of the valve through the inlet Fig 2.

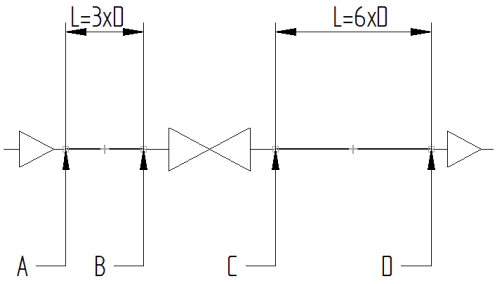

Fig. 2. Flow test scheme (ISA 1996)

The simulations are carried out under normal conditions, with an atmospheric pressure of 1,013 bar and a temperature of 20,05 °C. The inlet port is set to a pressure of 10 bar, and the pressure in the output is changed in 1 bar increments, from 1 to 9 bar.

To harmonize flow, and according to the standard, the inlet 3xD and output 6xD are inserted into the valve and outlet openings, where D is the diameter of the pipe. The diameter of the pipe D = 19 mm is used because it is also the internal diameter of the inlet and outlet thread G1/2, and this allows us to directly assess the valve capability by eliminating obstacles due to joints and transitions. The following parameters are measured:

a. average mass flow;

b. average flow rate;

c. average gas density;

d average gas temperature.

Parameter *a* is used for control since the mass flow rate must remain constant throughout the cross-section of the valve. It should be taken into account that there may be differences in the mass flow rates, as the used calculation power is limited to perform the simulation and therefore the density of the calculation matrix is also limited. Parameters *b*, *c* and *d* are used to calculate volumetric flow under normal conditions. The flow rate is calculated using the ideal gas law (1).

$$\frac{p \cdot V}{T} = n \cdot R \tag{1}$$

By elaborating equations 2, replacing the pressure, volume and temperature in one case with the normal conditions and, in the second case, with the measured results, and then equating the equations (since *nR* must be constant), we get the equation 2.

$$V_1 = V_2 \cdot \frac{p_2}{p_1} \cdot \frac{T_1}{T_2} \tag{2}$$

By replacing the volume of gas in this equation with flow, we can calculate the flow in normal litters per minute in formula 3.

$$Q_n = Q \cdot \frac{p_2}{p_n} \cdot \frac{T_n}{T_2} \tag{3}$$

where, Q_n – is the flow rate under normal conditions, NL/min,

Q – flow rate, L/min,

p_2 – pressure, bar,

p_n – pressure under normal conditions, bar,

T_n – temperature under normal conditions, K,

T_2 – temperature, K.

To find a characteristic line, the average flow rate for all cross sections is calculated and a graph is drawn up. The indicator capacity graph is also used to estimate valve capacity. The indicator power is calculated as the multiplication of the average pressure passing through the cross section of the valve and the average flow rate passing the cross section of the valve, and is presented in the equation 4. This equation is derived from the unit of power W.

$$P_i = Q_i \cdot p_i \tag{4}$$

where, P_i – indicator power , W,

Q – flow rate in cross section, L/min,

p_i – pressure in cross section, bar.

Valve efficiency is calculated using formula 5. The formula is based on a well-known principle in physics, where the system's efficiency is proportional to the input-output ratio.

$$\eta = \frac{P_A - P_D}{P_A} \cdot 100\% \tag{5}$$

where, P_A – indicator power in cross section A, W,

P_D – indicator power in cross section D, W,

η – efficiency, %,

Figures in the cross-section of the valve are also formed to illustrate the gas pressure, speed and Mach number.

3. CD12 VALVE ANALYSIS

The valve was disassembled and the necessary measurements were made to create a 3D model for the CD12 Valve. The model was designed to perform in the simulations with sufficient details and accuracy. Therefore, only the valve body and spool were modelled (Fig. 3.)

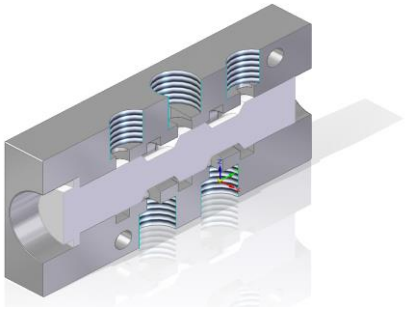

Fig. 3. Flow test scheme

The CFD analysis was performed to evaluate the capacity of the valve. The test scheme is shown in Fig. 4.

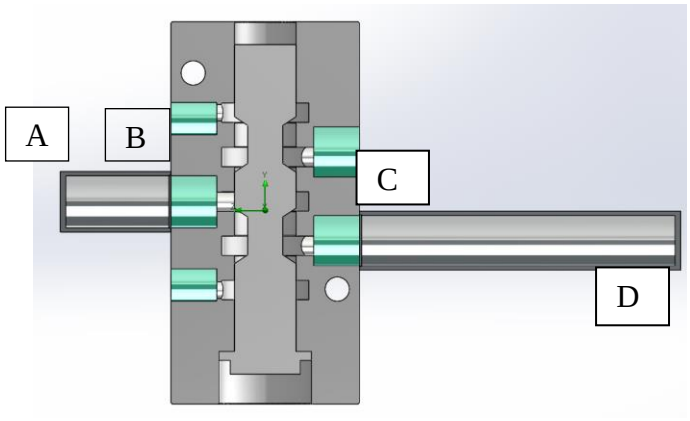

Fig. 4. Test scheme of the CD12 valve

The FloEFD built-in functionality for automatic refinement of the matrix was used to provide sufficient matrix accuracy. The refined simulation matrix is shown in Figure 5.

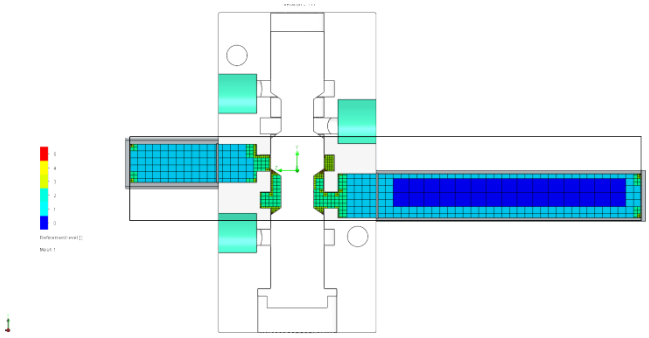

Fig. 5. **S**imulation matrix of the CD12 valve

Based on the analyse results, illustrative drawings were made to describe the velocity and pressure of the airflow in the valve cross-section at an output pressure of 1 bar (Fig. 6-7).

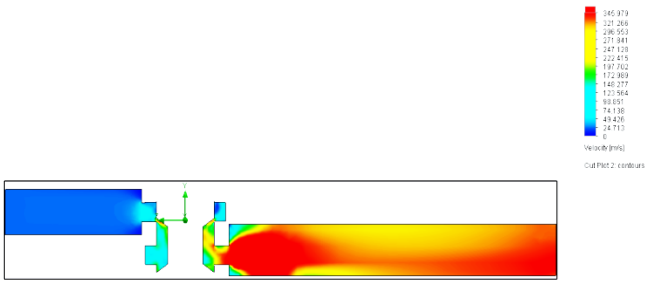

Fig. 6. Flow rate change in flange cross-section at 1 bar output pressure

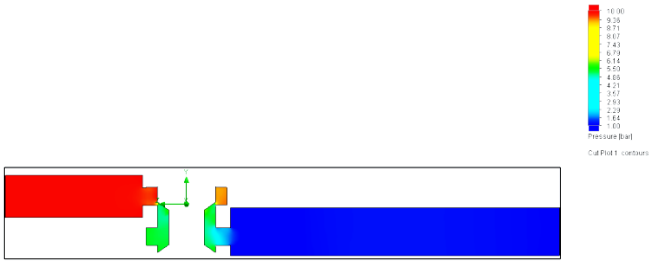

Fig. 7. Pressure change in the valve cross-section at 1 bar output pressure

The mass flow through the valve cross sections is shown in the graph in Fig. 8.

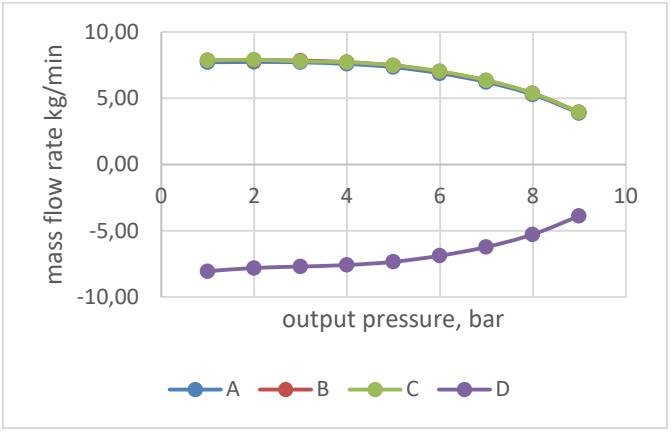

Fig. 8. Mass flow rate in valve sections A...D

The normal flow rate in the valve sections A…D is shown on the graph in Fig. 9.

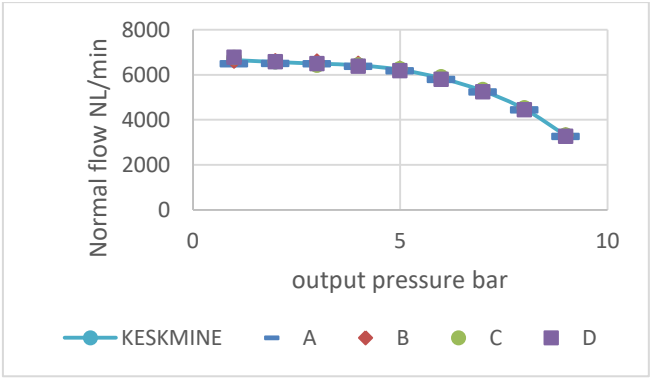

Fig. 9. Normal flow in valve sections A...D

The indicator power in the valve cross sections A...D is shown in Table 1. and in Fig. 10.

Table 1. Indicative power in valve sections A...B

Output pressure, bar	1	3	5	7	9
A	10,8	10,8	10,3	8,7	5,4
B	11,0	11,0	10,5	8,9	5,5
C	7,1	9,7	10,1	8,8	5,5
D	9,2	10,5	10,2	8,7	5,4

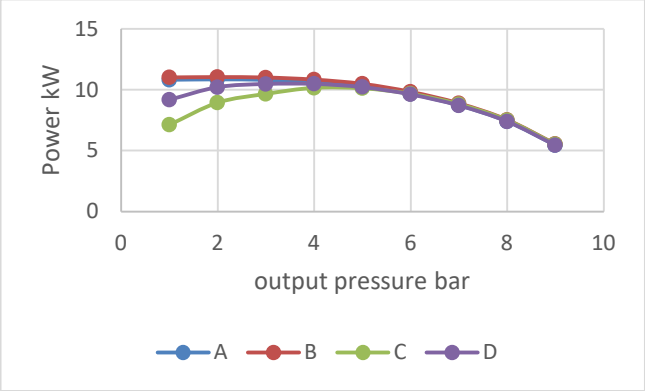

Fig. 10. Indicator power in valve cross sections A…D

It can be seen from the graphs that in the ratio of inlet and outlet pressure between 1 and 0.5, both mass flow and volumetric flow in normal litter units per minute remain unchanged through the valve substantially. In addition, based on the indicator power curve, it appears that the highest efficiency is ensured in the range of 4 to 9 bar output pressure. In the range of 1 to 4 bar output pressure, the output power is significantly lower than the input power, which results in a reduction in the amount of energy that can be transmitted in that area.

The theoretical efficiency of the valve is given in Table 2 and in Fig. 11. it is calculated with the equation 5.

Table 2. valve efficacy

Output pressure, bar	1,0	3,0	5,0	7,0	9,0
Efficacy, %	84,9	96,9	99,2	99,8	100,0

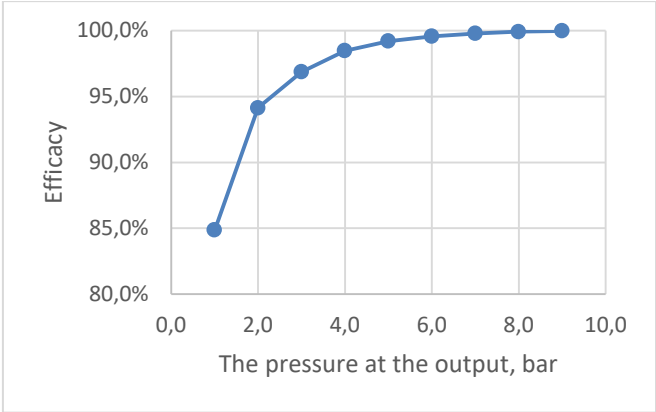

Fig. 11. Valve efficacy

The figure describing the efficiency of the valve and the table shows that the maximum efficiency is achieved at an output pressure of 9 bar, and the valve is most effective in the range of 5 to 9 bar, which is why it is wise to use a valve in a system with a flow of ~ 6200 L/min without a greater pressure drop than 5 bar.

Based on the analysis and the illustrative drawings in Appendix B, it appears that it is expedient to design a new valve with a smooth flow path as possible, and it is evident that abrupt constraints cause the gas velocity to change to a supersonic-speed.

4. PROTOTYPE VALVE CFD ANALYSIS

The new valve is designed as a 2x2 / 2 valve, which allows both the inlet and outlet to be independently controlled. The switches are implemented by applying a pilot pressure to the sides of the switch piston. The valve consists of three main parts: inlet module, outlet module, and divider. Aluminium is used as material. The airtight connections between the details are sealed using O-rings.

The seal between the sealing piston and the valve body takes place between the 45 ° phase and the compressed o-ring.

The valve was modelled with Solid Edge ST10 drawing software. The isometric view of the valve's 3D model is shown in Fig. 12. The valve consists of six basic details, shown in Fig. 13. of the valve cross-section.

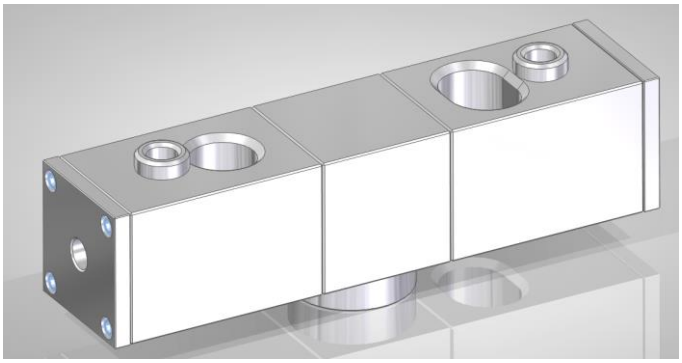

Fig. 12. Valve 3D model

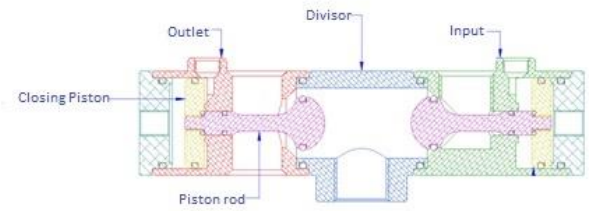

Fig. 13. Valve cross-section

The CFD analysis was performed to evaluate valve capacity. The test pattern is shown in Fig. 14.

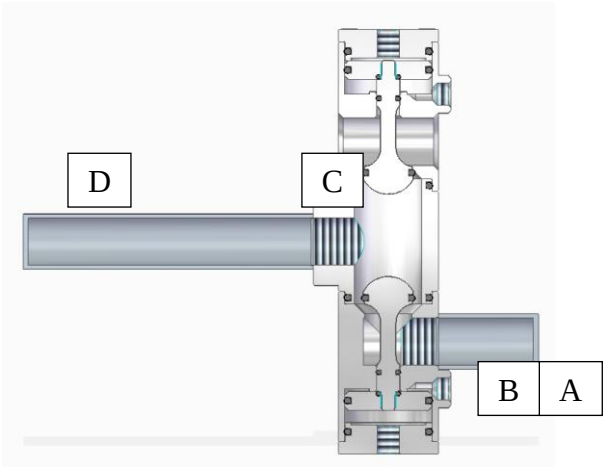

Fig. 14. Test pattern for prototype valve

A refined simulation matrix is shown in Fig. 15.

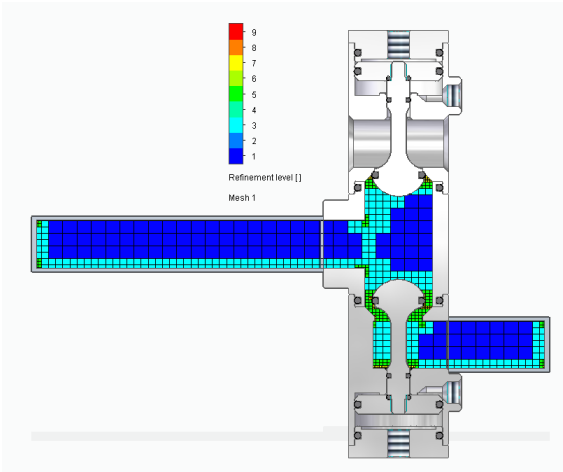

Fig. 15. Prototype valve analysis matrix

Based on the test results, illustrative drawings were made to describe the air flow velocity, pressure and mach number in the valve cross-section at an output pressure of 1 bar (Fig. 16-17).

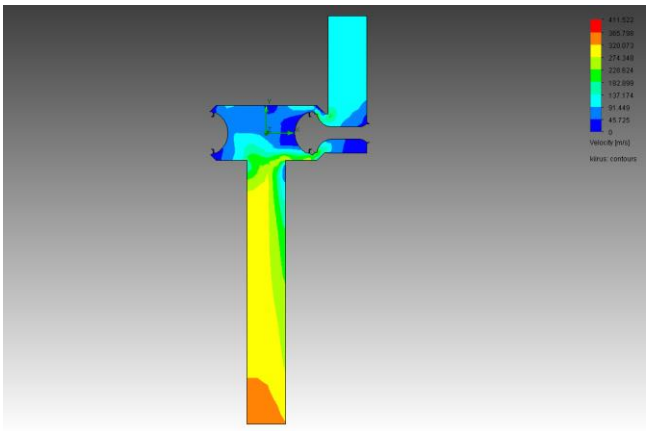

Fig. 16. Flow rate change in flange cross-section at 1 bar output pressure

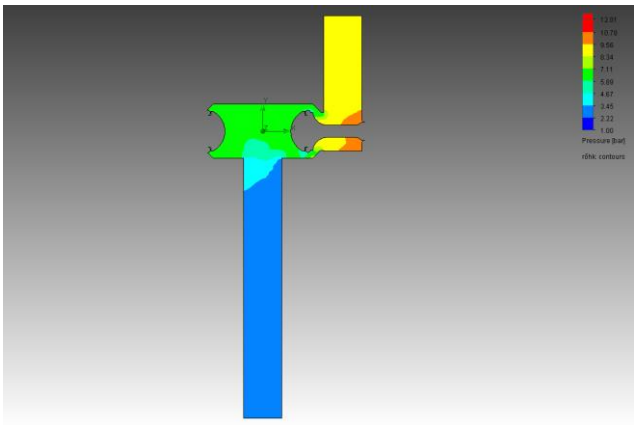

Fig. 17. Pressure change in the valve cross-section at 1 bar output pressure

The mass flow through the valve cross sections is shown on the graph in the Fig. 18.

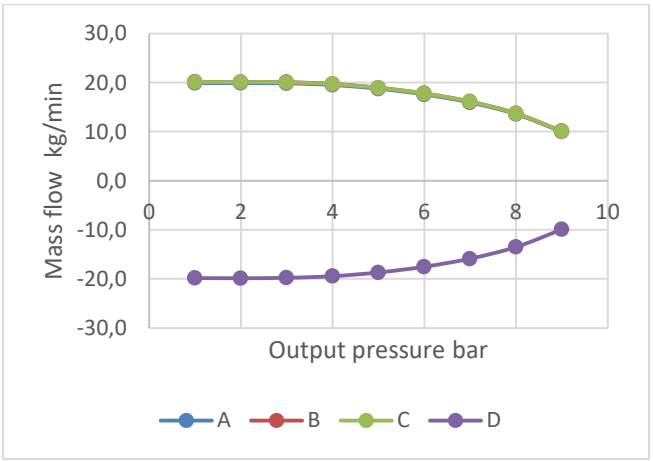

Fig. 18. Mass flow in valve sections A...D

The normal flow rate in valve sections A...D is shown on the graph in Fig. 19.

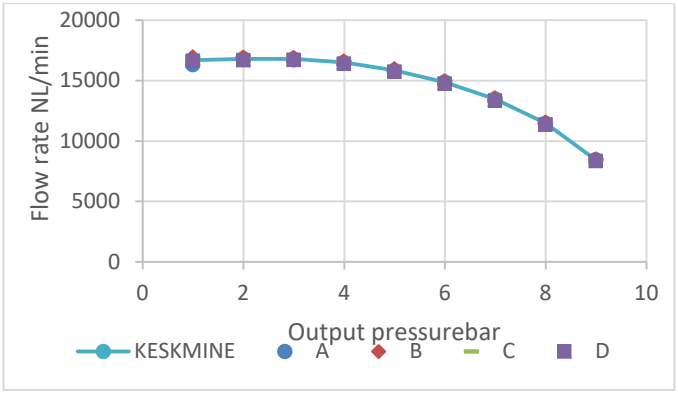

Fig. 19. Normal flow rate in valve sections A...D

The indicative power in the valve sections A...D is shown on the power curve is in Fig. 20.

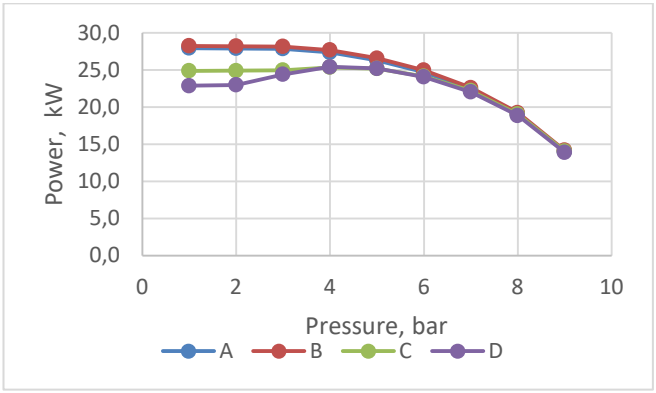

Fig. 20. Indicative power in valve sections A...D

It can be seen that, in response to the indicator power curve, the highest efficiency is guaranteed in the range of 7 to 9 bar and also with output pressure greater than 9 bar. It can be assumed that at an output pressure of 9 bar ≤ p <10 bar an equivalent or higher flow rate is ensured, with higher efficiencies than for the valve CD12.

The theoretical efficiency of the valve is given in Table 3 and in Figure 21, calculated with the equation 5.

Table 3. Valve efficiency

Output pressure, bar	1,0	3,0	5,0	7,0	9,0
Efficiency, %	81,9	87,7	95,8	98,6	99,2

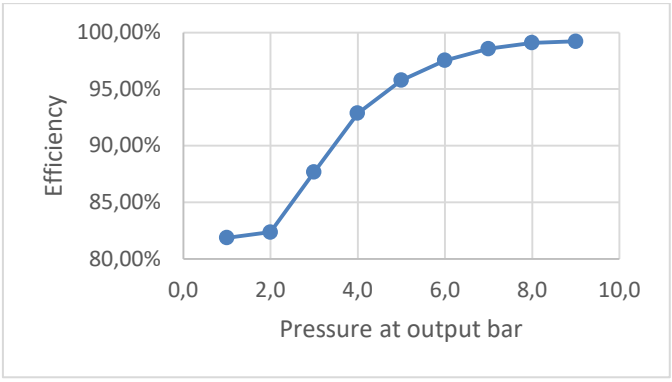

Fig 21 Valve efficiency

From the graph and the table, it is seen that the maximum efficiency is achieved at an output pressure of more than 7 bar, with a flow rate of 13470 NL / min. At ~ 2.55 times the flow rate is guaranteed under the given output conditions. While the prototype valve system can only provide a 1.2% lower efficiency.

Therefore, it is theoretically possible to provide both greater system power and efficiency at the same flow rate.

5. RESULTS AND DISCUSSION

For the comparison of the two valves, the data from the analysis are presented in Table 6.1.

Table 4. Comparative data of the valves

Valve	Flow rate	Mass
CD12	6655 NL/min	1 kg
Prototype valve	16810 NL/min	0,5 kg

Goals consistent with metrics have been achieved. To validate solutions, the prototype needs further testing. Resistance should be tested and valvular bandwidth evaluated.

6. CONCLUSIONS

According to the initial task, the CD12 analysis of the valve was performed using the CFD method. Based on the analysis, the prototype valve was designed in a configuration that allowed testing of technical solutions. It also analyzed the valve throughput and concluded that this design was justified. Based on practical experiments, weaknesses in the valve were identified and solutions to the problems were solved.

Subsequently, a 2x2 / 2 valve was designed and constructed. The valve was analyzed by the CFD method and concluded that the valve has significantly higher permeability and greater efficiency than the compared CD12 valve equivalent flow.

REFERENCES

„Aventics,“ Aventics, [Võrgumaterjal]. Available: https://www.aventics.com/de/en/pneumatics-shop/series-cd12-pgr.259999. [10.12. 2018]

ISA, Control Valve Capacity Test Procedures, ISA, 1996

ISA, Flow equations for sizing control valves, ISA, 2007.

J. F. Wendt, Computational Fluid Dynamics, 1995.

M. S. James A. Davis, „Predicting Globe Control Valve Performance—Part I: CFD Modeling,“ ASME, 2002.

Swagelok, „www.swagelok.com,“ swagelok, 12 2007. [Võrgumaterjal]. Available: https://www.swagelok.com/downloads/webcatalogs/EN/MS-06-84.PDF. [Kasutatud 12 11 2017].

Adaptive control based air expansion range extension of pneumatic vehicles

Zoltán Márton*; Dénes Fodor**

** University of Pannonia, Faculty of Engineering, Institute of Mechanical Engineering, Department of Automotive Mechatronics, 8200, Hungary (e-mail: marton.zoltan@mk.uni-pannon.hu)*
*** University of Pannonia, Faculty of Engineering, Institute of Mechanical Engineering, Department of Automotive Mechatronics, 8200, Hungary (e-mail: fodor@almos.uni-pannon.hu)*

Abstract: The annually held international Pneumobil competition organized by Aventics Hungary Ltd. has different race categories. One of these categories is the distance race. To achieve longer driving distance with the same amount of compressed air the efficiency of the cylinder must be improved by taking advantage of compressed air expansion. Its downside is that the torque and speed of an engine using pneumatic cylinders will vary depending on the position of the pistons. Under high load this can cause the engine to stop. In this paper an adaptive control algorithm is proposed which prevents engine stalls and facilitates optimal air usage. The algorithm requires the position measurement of the piston and the pressure data in the active cylinders. From these it can estimate the load and calculate the piston position from where the expansion should be used. If the algorithm detects engine stall then the pneumatic valve will be reopened until the piston accelerates to an estimated speed. To avoid the same situation in the next cycle the value of a factor which is responsible for the expansion starting position calculation will be increased. If the piston speed is faster than the estimated speed then this factor is decreased. The results were in concordance with the expectations.

1. INTRODUCTION

In case of the currently wide spread control of the pneumatic cylinders the pressure during the whole stroke develops according to the load which includes the exhaust flow control. When the cylinder reaches the end position the pressure quickly increases to the supply pressure. Because of this the air usage and efficiency of the pneumatic cylinder is not optimal. In the industry, where the compressed air is always available, this is usually not an issue but in a pneumatic vehicle, where only a given volume of compressed air is available, it is essential how the available air is used. The creation of the compressed air requires energy which should be regained during the expansion of compressed air (Rahul Kumar et al.). For example in a pneumatic cylinder if the supply air flow is closed before the cylinder reaches its end position the cylinder will continue its movement. Since the pressure is decreasing the force and the torque will decrease simultaneously. If the load is bigger than the current torque of the pneumatic cylinder engine the vehicle may stop. Different techniques are available to avoid this. It is important to remark that none of those techniques will utilize the full energy of the compressed air during expansion because of the losses inside the system, so some overpressure in the cylinders must remain in the system before changing the direction of the piston movement.

1.1 Overview of the existing solutions

There are different solutions to prevent a pneumatic cylinder engine stall. One method is to build such an engine configuration where the driving shaft is always rotating in the same direction regardless the direction of the cylinder movement. When engine stall is detected to prevent the vehicle from halting it is enough to switch the direction of the movement. In this case the achievable air consumption will be higher than the optimal because the piston does not reach the end position. During the direction change a relative high volume must be filled with pressure high enough to start move the piston in the opposite direction. The Pneumobil team of The University of Pannonia implemented this method in their first racecar back in 2016 but they decided not to use it during the race because test results were not too promising. A different approach is to use similar structure like the common 2 stroke combustion engine. With the right tuning the efficiency of the engine is between 65% and 75%. (Abhishek Lal). Some researchers suggest that the intake valve should be opened from crank angle of 0° and closed at 150°. The exhaust valve should be opened at the crank angle of 170° and closed at 340° (Chih-Yung Huang et al.). With that setting, according to their results, at air supply pressure of 9 bars the exhaust pressure does not exceeds 2.5 bars. This could be improved further if the valve opening and closing scheme is optimized for the distance race. Since the racetrack does not contain any up hills or down hills, the controlling of the cylinder can be preset in a way to use the compressed air expansion to a bigger extent. This is perfect for the distance race but a general solution for the problem requires a real-time control algorithm (Zhenggang et al.).

2. OUR PREVIOUS SOLUTION

Our pervious solution is similar to that of Zhenggang Xu and Xiaopeng Xie's published in 2009 but it was developed independently. These controlling algorithms need constant cylinder pressure and position monitoring. Furthermore, a simplified pneumatic cylinder model is required. To create a simplified model first the fluid dynamics must be neglected and only the pressure-force relations have to be used. The movement of the piston can be described as seen in equation (1).

$$\frac{d^2x}{dt^2}m + F_S + p_aA = (p_a + p')A \tag{1}$$

where x denotes the distance measured between the air supply and the piston position, m is the moved mass by the cylinder, Fs denotes all the losses in the system, A is the active surface of the piston, which does not include the surface of the piston rod, pa stands for the external air pressure and p' is the current overpressure. As the external air pressure affects both sides of the piston the terms containing the external air pressure can be neglected resulting in a simpler equation (2).

$$\frac{d^2x}{dt^2}m + F_S = p'A \tag{2}$$

Suppose that after the piston reaches a given x0 position the air supply is closed and the compressed air is sealed inside the cylinder. Then, the overpressure in the cylinder is p0' and using equation (1) following interrelations can be formed.

$$V_0 = x_0A \tag{3}$$

$$V = xA \tag{4}$$

$$p_0V_0 = pV \tag{5}$$

$$p = p_0\frac{V_0}{V} = p_0\frac{V_0}{xA} \tag{6}$$

$$pA = \frac{d^2x}{dt^2}m + F_S \tag{7}$$

$$p_0\frac{V_0}{xA}A = \frac{d^2x}{dt^2}m + F_S + p_aA \tag{8}$$

$$\frac{p_0V_0}{x} = \frac{d^2x}{dt^2}m + F_S + p_aA \tag{9}$$

$$p_0 = p_a + p_0' \tag{10}$$

These relations can be then used to form (11) and (12):

$$(p_a + p_0')\frac{V_0}{x} = \frac{d^2x}{dt^2}m + F_S + p_aA \tag{11}$$

$$\frac{1}{x} = \frac{\frac{d^2x}{dt^2}m + F_S + p_aA}{(p_a + p_0')Ax_0} \tag{12}$$

where beside our previously used legends p0' is the initial overpressure, p is the current absolute pressure, V0 denotes the initial volume of the air supply side of the cylinder, x0 is the initial and x is the current position of the piston. First the position needs to be estimated from which the piston can reach the end position utilizing only the energy obtained from the expansion of the compressed air. Since the end position is the position for the direction change it is acting like an inflexion point so the acceleration is exactly zero, which allows us to leave out the first term of the equation (11)'s right side. Furthermore, it is important to remark that in this case the external air pressure cannot be neglected because when the air is sealed in too early then at the air supply side of the cylinder vacuum will occur which will act like a brake to the system. During the building of a pneumatic vehicle if we want to be cost-efficient we can avoid the utilization of an absolute external air pressure sensor (barometer) by assuming the external air pressure to be always exactly 1 bar. In this case equation (13) can be obtained.

$$\frac{1}{l} = \frac{F_sA \cdot 1\,bar}{(1\,bar + p_0')Ax_0} \tag{13}$$

where l denotes the length of the stroke. From the equation above the dependence of the exact position of the optimal compressed air expansion utilization (x0) on the losses (Fs) can be observed. To obtain these losses a further sensor built in the piston would be required which would raise the costs and make the building of such a system more complicated. Another option is to expand our controller with engine stall detection and prevention features. Under these conditions the losses can be neglected and our previous equation is reduced (14).

$$x_0 = \frac{1}{(1 + p_0')} \tag{14}$$

where p0' is the overpressure measured in bars. At the startup the algorithm initializes and starts a timer which is used to sample the overpressure inside the active half of the pneumatic cylinder and the position of the piston. For each timer tick the value of x0 is calculated and compared against the current position. When the position of the piston has passed the calculated value the algorithm switches to a different calculation mode. First, it calculates the average speed of the piston and estimates the position of the piston at the next timer tick. After that the current position of the piston is compared to the previously estimated value for each timer tick until the direction change. At the end of the cycle the next expected position is re-estimated. If the measured position is before the estimated then it takes on action. But if it is after then the algorithm is switched into the engine stall prevention execution mode and the air supply valve which sealed the compressed air in the cylinder is re-opened. After that for each tick the system is testing the piston position. If it surpasses the estimated position the valve is closed again and

the algorithm returns to normal execution mode. If the piston reaches the end position then the direction is switched and the algorithm is restarted.

Since we inherited the vehicle built by the previous team for the 2017's Pneumobil Race it lacked the sensors and tools required or the present ones were not suited to implement this algorithm (Figure 1 and 2). For example there were no pressure sensors connected to the cylinders and only eight reed relays was present to monitor the piston position. The algorithm was later implemented for this vehicle but it was only finished after the race so it could not be used during the distance race. The tests were done in simulations.

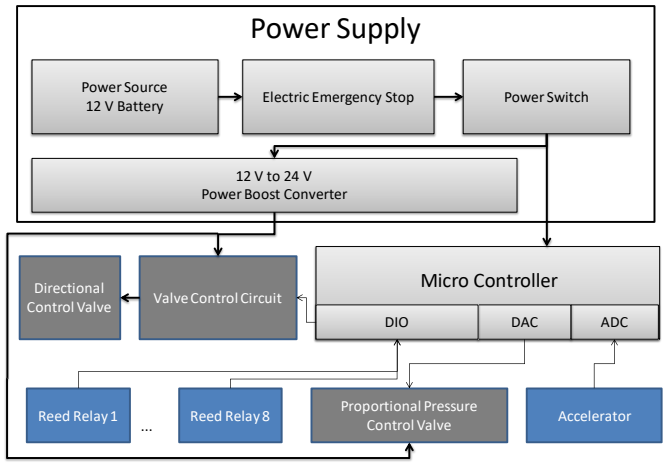

Fig. 1 the controlling system of the inherited vehicle

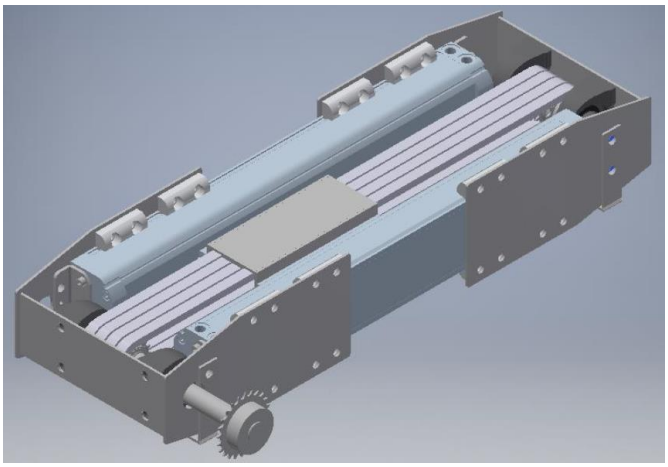

Fig. 2 the driving system of the inherited vehicle

3. THE PROPOSED SOLUTION

In the past year the control algorithm was improved. A new factor was introduced which is applied to minimize the times the intake valve is re-opened and re-closed during the piston movement. The essence of this new algorithm is the same as that of the old one but an important difference is that the newly introduced factor is used in the calculation of x0 as shown in equation (15). The factor is initialized to 100% when the piston movement is started for the first time. If engine stall prevention is activated then the factor is increased by a given value and the reduction of the factor is disabled. If the difference between the estimated and the real (current) piston position is twice as much as the increase used for estimating the next position and the factor decreasing is allowed then the factor will be decreased by a given value. Thus, the controlling algorithm can adapt itself to the current load of the piston. The factor is prevented to go below 90%.

$$x_0 = f\,\frac{1}{(1+p_0')} \tag{15}$$

4. SIMULATION AND RESULTS

The new advanced algorithm has not been tested yet but the previous one was tested in simulations. Unfortunately, the available FluidSym software was not capable of simulating compressed air expansion thus the following test system was built (Figure 3). The exhaust flow control was used as a load of the pneumatic cylinders.

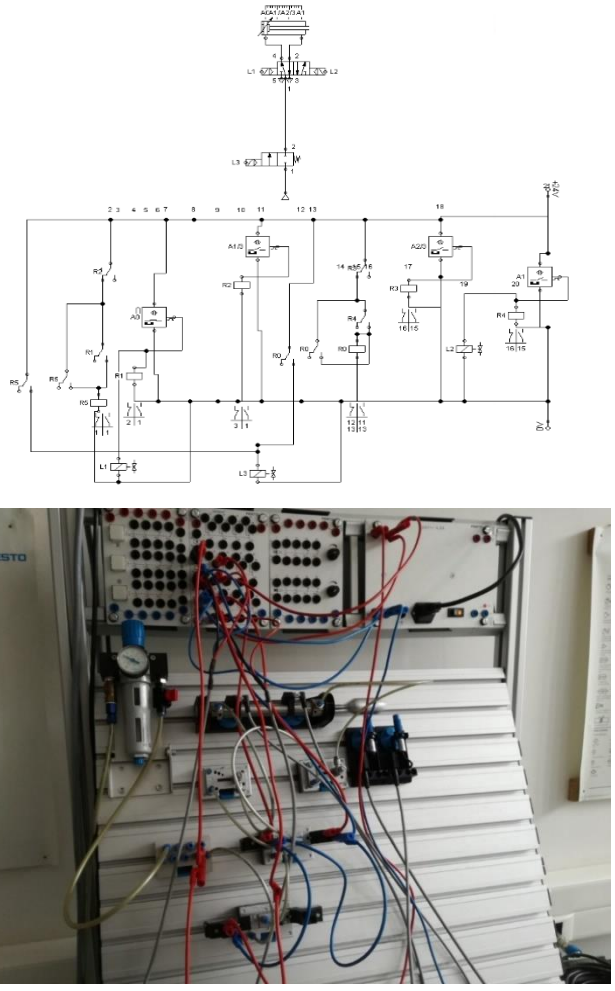

Fig. 3 a., the pneumatic and electric scheme of the test system; b., the built test system

Under the given circumstances the following results were obtained (Table 1). Since the test system utilized direct electrically controlled valves the air supply pressure could be lowered below 3 bars. Later the algorithm was adapted and implemented for the previously built pneumobil vehicle and was tested on it successfully. The pistons were accelerating till the end positions without load. With load the pistons were moving at a roughly constant speed and under overload the algorithm successfully prevented engine stalls.

Table 1. The measured results on the test system

p_0' [bar]	x_0/l
6	25%
5	30%
4	33%
3	45%
2	60%
1	unstable

5. CONCLUSIONS

Our previous algorithm is capable of utilizing compressed air expansion without engine stall. The advanced algorithm will be tested on our new vehicle. Since the previous vehicle did not utilize any kind of air expansion method during the races so we are expecting a much better result in the distance race. The adaptive nature of the new method sets expectations to have a lower air usage then the old one but this is expected to be proven during the race. To further advance this algorithm we should expand it with a loss estimation method.

ACKNOWLEDGEMENT

This research is supported by EFOP-3.6.1-16-2016-00015 project. The project is supported by the Hungarian Government and co-financed by the European Social Fund.

The project has been supported by the European Union, co-financed by the European Social Fund. (EFOP-3.6.2-16-2017-00002).

REFERENCES

Abhishek Lal, Design and Dynamic Analysis of Single Stroke Compressed Air Engine, INTERNATIONAL JOURNAL of RENEWABLE ENERGY RESEARCH, **Volume 3**, No.2, 2013

Chih-Yung Huang, Cheng-Kang Hu, Chih-Jie Yu and Cheng-Kuo Sung, Experimental Investigation on the Performance of a Compressed-Air Driven Piston Engine, Energies 2013, Issue 6, 1731-1745, ISSN 1996-1073, doi:10.3390/en6031731

Rahul Kumar and Anand M G, Simulation and construction of Single-stage reciprocating pneumatic transmission system Engine, International Journal of Scientific and Research Publications**, Volume 2,** Issue 7, July 2012, ISSN 2250-3153

Zhenggang Xu and Xiaopeng Xie, A method for reducing exhaust pressure of vehicle compressed air powered engine, **Mechatronics and Automation, 2009., IEEE ICMA 2009**. International Conference, ISBN: 978-1-4244-2692-8, DOI: 10.1109/ICMA.2009.5246632

Analysis of the Rolling Resistance of Pneumobiles for Vehicle Dynamic Modelling Purpose

Bence Márk Szeszák *, György Juhász **, GusztávÁron Sziki *, Rita Nagy-Kondor****, Tamás Sádor Sütő *******

**University of Debrecen, Faculty of Engineering, Department of Mechanical Engineering, 2-4 Ótemető Street, Debrecen, H-4028, 0036202499574, szeszakbence@gmail.com*

*** University of Debrecen, Faculty of Engineering, Department of Mechanical Engineering, 2-4 Ótemető Street, Debrecen, H-4028, juhasz@eng.unideb.hu*

**** University of Debrecen, Faculty of Engineering, Department of Basic Technical Studies, 2-4 Ótemető Street, Debrecen, H-4028, szikig@eng.unideb.hu*

***** University of Debrecen, Faculty of Engineering, Department of Basic Technical Studies, 2-4 Ótemető Street, Debrecen, H-4028,rita@eng.unideb.hu*

****** University of Debrecen, Faculty of Engineering, Department of Mechanical Engineering, 2-4 Ótemető Street, Debrecen, H-4028,suto.tamas28@gmail.com*

Abstract: In our previous publication we presented a vehicle dynamic model for pneumobiles and also described a simulation program that is based on this model and was developed in MATLAB environment. One of the input parameters of the program is the rolling resistance coefficient of the tyres. The present publication describes the experimental set-up and work in the course of which the above coefficient was measured and the effect of tyre pressure on rolling resistance was analyzed.

1. INTRODUCTION

In our previous study the motor characteristics curve of a self developed pneumobile was determined and the motion of equation of the vehicle was solved. A simulation program for the calculation of the vehicle dynamic functions of the mobile from its technical data has been also developed in MATLAB environment. One of the required input parameters of the program is the rolling resistance coefficient of the tyres. Figure 1 shows the different forces acting on the mobile during its motion.

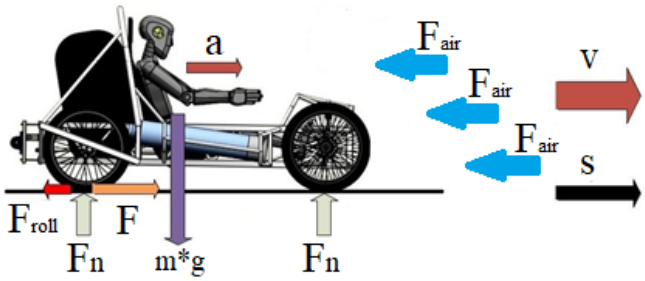

Figure 1. Forces acting on the mobile

On the bases of *Figure 1* the motion of equation of the pneumobile is as follows:

$$\sum_i F_l = F(v) + F_{roll} + F_{air} = m \cdot a \qquad (1)$$

In the above equation F_{roll} is the rolling resistance which is calculated by the following formula:

$$F_{roll} = c \cdot m \cdot g \qquad (2)$$

where$c$ is the rolling resistance coefficient of the tyres and m is the mass of the vehicle together with the driver. In the recent publication the measurement process of the above coefficient vs. tyre pressure – together with the obtained results – is presented.

2. MATERIALS AND METHODS

The applied measuring system - which is built up of five subunits - is shown in *Figure 2.*

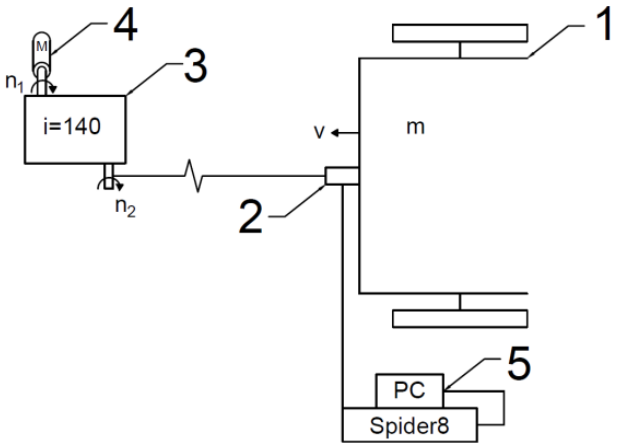

Figure 2. Schematic view of the measuring system

1. *Pneumobile:* We performed the measurements on that vehicle.

2. *Load cell:* The load cell was fixed to the vehicle by an M5 threaded stem firmly. To the load cell a tow rope was attached through a self made threaded sleeve to ensure the cell's one axle loading which is a prerequisite for precise measurement.

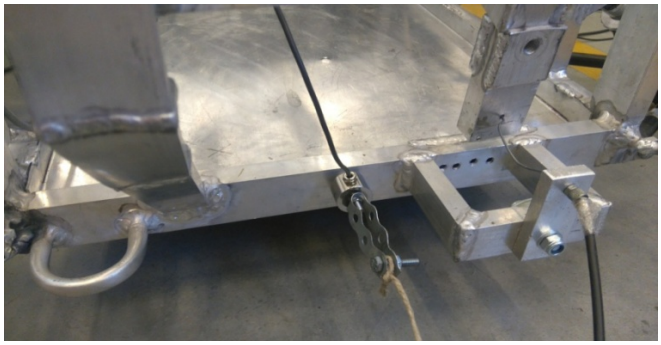

Figure 3. The load cell

3. *Worm gear:* To ensure an adequate and constant traction force, thus velocity, the tow rope was pulled by means of a worm gear. The worm gear was fixed to a wooden base firmly to ensure its stability.

Figure 4: The worm gear

4 *Drive:* The worm gear was driven by a Metabo SBE570 type electric drill. The drill was operated at its maximum angular speed of 3000 [1/min].

5 *Electronics and PC:* A Spider8 multi-channel PC measurement electronics was applied using it with its own software.

3. RESULTS

The coefficient of rolling resistance of a loaded pneumobile (weight of 650 N) has been measured at 13 different tyre pressures between 1 and 7 [bar] in 0.5 [bar] steps. At each pressure 10 measurements were made, and the average and standard deviation of the data were calculated. The obtained results are presented in *Table 1* and *Figure 5.*

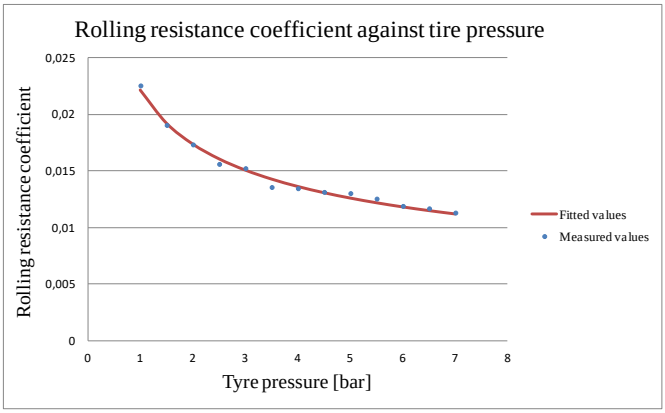

Figure 5: Rolling resistance coefficient against tyre pressure

The model function below was fitted to the measured data (*Figure 5*) applying Maple13 software.

$$c(p) = A \cdot p^{-B} \quad (3)$$

In the above formula A and B are parameters calculated by Maple13. It has to be emphasised here, that the fitting procedure can be also performed by MATLAB. The authors used Maple13 because a ready-to-use Maple13 program was available for them.

4. CONCLUSION

The coefficient of rolling resistance of a loaded pneumobile has been measured at 13 different tyre pressures between 1 and 7 [bar] in 0.5 [bar] steps. The model function recommended in reference has been fitted well to the measured data. The above function – or the original data in the form of "Look up table" – will be built into our MATLAB/SIMULINK program enabling the calculation of rolling resistance coefficient directly from tyre pressure. In the near future we intend to study also the effect of load on rolling resistance coefficient.

Table 1. Measured rolling resistance coefficients at different tyre pressures

Pressure [bar]	1	2	3	4	5	6	7	8	9	10	Avarage	Standard deviation
1	0,021997	0,022533	0,02307	0,021996888	0,021997	0,022533398	0,02307	0,02307	0,022533	0,022533	0,022533398	0,000438058
1,5	0,018778	0,019314	0,018241	0,019314341	0,018778	0,018777831	0,019314	0,019314	0,018778	0,019851	0,019046086	0,000455945
2	0,017168	0,017705	0,017705	0,018241322	0,017168	0,017168303	0,017705	0,016095	0,016632	0,017705	0,017329256	0,000622084
2,5	0,016095	0,015559	0,016632	0,015558775	0,015022	0,015022265	0,015559	0,016632	0,015022	0,015022	0,015612426	0,000642319
3	0,014486	0,015022	0,015022	0,016095284	0,015559	0,015558775	0,015022	0,015559	0,014486	0,015559	0,015236869	0,000518317
3,5	0,013413	0,013949	0,013413	0,012876227	0,013949	0,013949246	0,013413	0,012876	0,013949	0,013949	0,01357369	0,000441694
4	0,013413	0,013413	0,013949	0,013412737	0,013949	0,013412737	0,012876	0,012876	0,013949	0,013413	0,013466388	0,000395871
4,5	0,013413	0,012876	0,013949	0,013412737	0,012876	0,012339718	0,013413	0,012876	0,013413	0,013949	0,013144482	0,000508978
5	0,013413	0,012876	0,012876	0,013412737	0,012876	0,012339718	0,013413	0,012876	0,013413	0,012876	0,01303718	0,000362116
5,5	0,012876	0,01234	0,012876	0,012339718	0,01234	0,012876227	0,011803	0,01234	0,012876	0,012876	0,012554322	0,000375131
6	0,011267	0,011803	0,011803	0,012339718	0,01234	0,011266699	0,01234	0,01234	0,011803	0,011803	0,01191051	0,000423204
6,5	0,011803	0,01234	0,012876	0,012339718	0,01073	0,011266699	0,011267	0,01073	0,011267	0,01234	0,011695906	0,000750261
7	0,01073	0,01234	0,01073	0,011803208	0,01073	0,010730189	0,011267	0,01234	0,011803	0,01073	0,01132035	0,000690318

REFERENCES

F. Grappe, R. Candau, B. Barbier, M. D. Hoffman, A. Belli, J.-D. Rouillon: Infuence of tyre pressure and vertical load on coefficient of rolling resistance and simulated cycling performance, ERGONOMICS, 1999, VOL. 10, 1361-1371

Juhász Botond (2014): Számítógépes program a pneumobil menetdinamikai paramétereinek számításához, TDK

Síki, G. Á., Juhász, Gy., Nagy-Kondor, R., Juhász, B.: Determination and Solution of the Motion of Equation of a Pneumatic Drive Vehicle

Veszelszki Krisztián, Szeszák Bence Márk (2016): Pneumobil gördülési ellenállásának vizsgálata, TDK

Szeszák Bence Márk, Sütő Tamás Sándor (2017): Pneumobil gördülési ellenállásának vizsgálata terhelt állapotban, TDK dolgozat

Human-electric hybrids and reaching times in commuting

János Bihari*, Ferenc Sarka**

**University of Miskolc, Miskolc-Egyetemváros 3515, Hungary*
(Tel.: +3620 9576 9992, machbj@uni-miskolc.hu)
***University of Miskolc, Miskolc-Egyetemváros, 3515 Hungary*
(Tel.: +36 565 111/12-47, machsf@uni-miskolc.hu)

Abstract. There are several researches that examine the traffic of European cities. The congestion level of cities cannot be ignored neither in logistical planning. The congestion of vehicles has a number of harmful public health and economic impacts. Most of the researches examine only the metropolises and their environment, but under certain conditions in smaller towns, like Miskolc, congestions can be formed and the access times rise in critical traffic periods. At the University of Miskolc at the Institute of Machine and Product Design researches on the design and the use of human-electric hybrid vehicles started in 2011. In the last few years the University is getting overcrowded. Consequently the access times rise also among the University and the parts of the town. This is why we feel that the examination of such vehicles should be linked to the measurement of access times. The price of the human-electric hybrid vehicles, like all the electric vehicles, is relatively high in their category. It goes with that such vehicles are not prevalent. So we would like to perform an experimental series. In this series we would like to analyze the limits, advantages and disadvantages of the real use of human-electric hybrid vehicle. The first part of the series was an experiment in May 2017. In this research students and professors of the University of Miskolc were participate. Relevant part of the examination was to collect user experiences. In this research the measuring of the access time was just for curiosity. The main purpose was how to collect and how to use the measured parameters.

1. HUMAN-ELECTRIC HYBRID VEHICLES

This group includes vehicles that are basically powered by human force and the drive is supported by one or more electric motors. So those scooters or mopeds that are equipped with pedals but they do not suitable for continuous driving by human force, belong to pure electric vehicles. The most common human-electric hybrids are e-bikes, pedeleces and s-pedeleces. They are built with two wheels and less often three or four wheels. We often meet electric bikes in Hungary.

1.1 Differences between the types of human-electric hybrid vehicles, legal background

1.1.1 Pedelec (Pedal Electric Cycle) EAPC

These kinds of vehicles have two or more wheels. The rider human is supported by maximum 250 W engine. The engine is working only then, when the human is pushing the pedals. If the vehicle reaches the 25 km/h (15.5 mph) speed, the engine switches off. These vehicles are capable to move faster than 25 km/h, but above 25 km/h rider should use own muscle force. These kinds of vehicles are counts as bicycle in most European countries (except Northern-Ireland) [1], [2], [3].

1.1.2 S- pedelec (Speed-Pedelec)

The working principle of S-pedeleces is the same of the pedeleces, but the engine help is available under 45 km/h speed. The maximum power of the engine is 4000 W. These kinds of vehicles are count as mopeds in most European countries, but in Hungary only then, when the power of the engine is greater than 300 W [3].

1.1.3 Electric bikes

These kinds of vehicles can move without human force, they are equipped with controls for adjusting power. The vehicle can be two or more wheeled. In most of European countries electric bikes have moped classification, but in Hungary only then, when they have more powerful engine than 300 W.

1.1.4 Other regulations

The human-electric hybrids are spreading and developing fast, and they have important role in the daily traffic. Nowadays there is a new variation of pedeleces, which have starter function. This function allows the user to start and drive the vehicle without any pedal force under 6 km/h. These kinds of pedeleces are popular among the older or weaker users. The above-mentioned vehicles are bicycles in Germany, Austria and Switzerland [2]

2. THE IDEA OF THE EXPERIMENT

In subjects about vehicles and traffic conditions the application of the vehicles must not be ignored. It is important to collect the experience and the interaction of students.

Reaching the University of Miskolc is getting harder and harder in peak hours by car. Parking problem is permanent; several cars are parking where it is forbidden students delay from the morning lessons, because of traffic problems. In this case the question arises whether the appropriate traffic way was chosen. Carefully think about this problem, we have to accept that it is hard to decide which is the appropriate traffic way. Majority uses such traffic opportunity that is reachable for them. Others make decision only on emotional basis. Then came up that it is worth to compare different traffic ways in same conditions while exclude all the emotional viewpoints. First of all, we measured with directed conversation why students use one or the other vehicle. We questioned students, how much time they usually spend with travelling to the University and which route they use. On the basis of the gathered information, we decided to make a test about access times. This test could be supplement of the theoretical examinations.

3. VEHICLES USED IN THE EXPERIMENT

We made several student groups on a voluntary basis. Typically, most of the students use public transportation or cars, but some use bicycle or motorcycle. None of them used human-electric hybrid vehicles even none of them tried one.

Fig. 1. One of the human-electric hybrids used in the experiment. The 250W engine is built in the front wheel the battery is in the box above the rear wheel.

In our Institute there are researches about human-electric hybrid vehicles. We chose two types of human-electric hybrid vehicles. Both are bicycles. One of them is a pedelec type the other is an electric bike with 250 W engine, which can be adjusted with a thumb-throttle (Fig.1.). One of these kinds of vehicle was driven by a person who has experience in cycling, the other one was driven by a person who can ride a bicycle but not used to. Besides that two students used his own conventional bicycles in the experiment. Another two teams used cars in the experiment and one team went by public transport. There were two other members of the experiment. One went by a moped and one went by motorcycle.

4. DETERMINATION OF THE ROUTE OF THE EXPERIMENT

The experiment was made in the time of education, so we had to choose such a route that can be done back and forth by any type of vehicle in two hours. Most of the students said that the greatest disadvantage of cycling is that cycling is not a safe way of transport, so we preferred closed cycling routes. At the same time, the traffic jams are forming the way from the city center to the University, so targets in the city center were also necessary. The final route had two targets. The first target was the statute of the rescue dog Mancs (Kazinczy street 2.), the second target was the Hall of Hungarian Academic Committee at the Erzsébet square. Students had to leave from Room 105, Building A1 of the University and they had to come back to the same place. They had to take photos at both targets, as evidence.

5. DETERMINATION OF ACCESS TIME

Many of us understand on access time those times that we spend with moving and waiting related to transport, although access time in urban transport can be more complex. In the experiment we considered the full access time: participants had to leave the classroom and had to get to the bus stop, or the parking place of their cars, or to the bicycle storage. Then they had to take their seats in/on their vehicles. They had to open the locks of the bicycles the motorcyclists had to get on crash helmets and protective gloves, and other similar activities.

Approaching the targets, they had to find parking places (had to pay for the parking) and do the remaining distance on foot at comfortable pace. If the participant used public transport it was important to choose the right bus stop. Every participant had to walk at comfortable pace during the pedestrian parts of their routes. All the participants had to observe the traffic regulations. With these rules the measured times meant the real access times and were comparable.

6. THE IMPLEMENTATION OF THE EXPERIMENT

Six teams were involved in the experiment, all of them on a voluntary basis. Two teams went by cars, one team went by public transport, one team went by conventional bicycles, one team by human-electric hybrids, one team used a moped and the last one used a motorcycle. All teams left the class room at the same time. Participants with conventional bicycles and participants with human-electric hybrids had to go with comfortable pace, not to get more tired than they would just walk.

Documentation of times was a problem from the beginning. The participants measured the time with stopper, but this way the stops could not be recorded. Teams used tracking

applications that could record stopping times but the reasons of stops were not recorded. As the used devices were not the same, not all the participants could use the same application (teams used their own devices). One team that went by car and the team that went by public transport used the same software. Data from these two teams were easily comparable.

The most important part of the experiment was the applicability of bicycles and human-electric hybrids in the traffic of Miskolc. These vehicles are well applicable if the average speed (including all additional times) that can be reached with them is higher than the public transport speed and not significantly lower than the speed of the cars. In case of bicycles the attainable speed depends on the physical condition of the cyclist but in case of human-electric hybrids within certain limits is independent from the physical conditions of the cyclist. This is the exact reason why can we change the car to human-electric hybrids on shorter distances.

The day of the experiment was 24.04.2017. Participants after a short coordination leaved the start point (Building A1, Room 105) at 12:06. The weather was nice and dry with a temperature about 20°C. The two teams with car did not park in the same place. One parked at Building A4 and the other at the Student Hostel E2. Both are a few hundred meters from the start point. Bicycles were locked in bicycle storage at the entrance of Building A4. The motorcycle and the moped parked behind Building A3 closer to the starting point than the cars. This situation is very specific to the parking possibilities; everyone parks where they have opportunity. The time of the experiment overlapped the Vehicle Elements lesson of the students. As this was the first experiment this time was favorable because in this period the traffic in the city center is moderate.

All teams chose the same route to the statue of Mancs. The route was the following: Miskolctapolcai street – Csabai gate – Görgei Artúr street – Szemere Bertalan street. Cars parked at the Arany János street, about three hundred meters from the statue. There were alternative routes to the other target (Erzsébet square) for those who went by public transport or bicycles (a closed bicycle route is at the edge of the square). Both of them went on the Széchenyi István street. This street is closed for motor vehicles. Cars used the only one way to the Erzsébet square, Uitz Béla street and then Kálvin János Street. Near the square mopeds, motorcycles and bicycles can park free, but cars must park a little further (about 150 m) and of course have to pay for parking.

The route from the city center to the University was the same for teams with bicycles, public transport and for one team with car. The other teams with motor vehicles chose the Hidegsor – Ruzsinszőlő – Csermőkei street – University route. One team got lost on the way back to the University.

Fig. 1. One of the teams at the statue of Mancs.

7. RESULT OF THE EXPERIMENT AND EVALUATION OF THE RESULTS

On the day of the experiment the motorcycle was the fastest vehicle. The reason of the fastest time is the simplicity of parking with motorcycle. Users of motorcycles spend less time with dressing up and down (glows, crash helmet, jacket) than car users spend with looking for parking places. On the routes of the city mopeds must go slower than the cars and if we take into account the simplicity of parking with a moped, the accessing time of the moped is the same as cars. The access time of the bikes were 50% longer then the access time of cars to the statue of Mancs, but was 50% shorter from the statue of Mancs to the Erzsébet square, because of the way opened for bicycles from the first target to the second. The access time with public transport is the longest among the examined vehicles. The distance between two bus stops is short, so we have to count with grate stopping times.

Table 1. The measured accessing times rounded to integer minutes

	Car 1	Car 2	HE hyb.	Motor-cycle	Moped	Public trans.
University – Statue Mancs	11	10	16	8	10	42
Statue Mancs – Erzsébet sq.	8	8	4	7	7	8 on foot
Erzsébet sq. – University	24 got lost	12	19	9	11	46

The circumstances of the examination were a bit too ideal, so we cannot make grounded conclusion. The weather conditions were very good; two wheeled vehicles could go without any impediments. The users of two wheeled vehicles are more careful in poor and slippery weather conditions. The traffic was moderate; car could go with the allowed speed, taking advantage of the green wave of traffic lights. We cannot find high rises on the route and the students use this

route often, so most of them have local knowledge. On the relatively flat way even the human-electric hybrids can reach higher speeds. We neither could determine how tired the cyclists were. We could only determine (not so scientific way) how sweaty or winded they were.

So this experiment is just a base of a series of experiments. With the use of the experiences we can make such a method that can give us useful date for the accessing times.

The users of the human-electric hybrids never used such a vehicle before this time. They often use cars in the city. All of them said they would use human-electric hybrids even instead of cars if they could pay the price of the hybrid vehicles.

The routes of the cars and the public transport can be seen in Fig. 3.

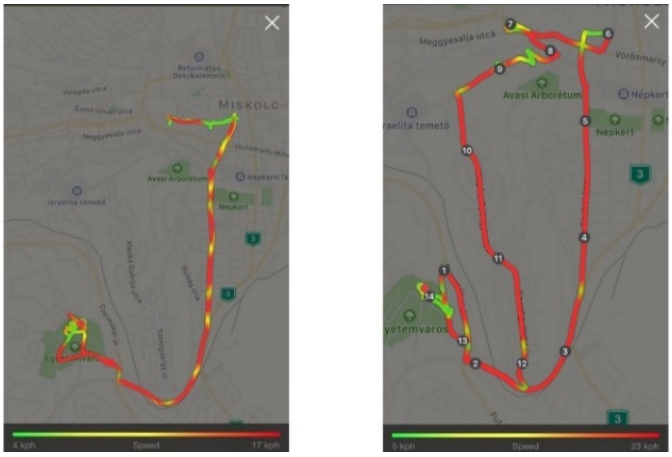

Fig. 2. Comparison of the route of the car (left) and the public transport (right). The lighter parts are the slower sections (stops or walking)

8. IMPORTANT EXPERIENCES FOR THE PERSPECTIVES OF LATER EXPERIMENTS

First, we have to unify the measuring of time and the recording of the routes. If we can realize this, the participants can record the data on their own in the daily routine. In this case not only the accessing times but costs can also appear among data. In our experiment we could determine that the pedelec used 4 Forints of electric energy, the e-bike used 5 Forints of electric energy. The determination of the consumption of the vehicles with combustion engine is harder than the case of bikes. It needs specific measuring devices. Incremental costs are also hard to determine. The one-way cost of the public transport is also hard to determine in case of season tickets.

In longer term it is worth to develop own application for this experiment. With a specific application we can sign fast and easily the reasons of the stops or obstacles. Recording the reasons of the stops with hand writing, or pushing buttons can be dangerous during driving. If we record a movie or just record sound, we can determine the reasons of the stops afterwards. Processing of the recorded movie can be time-consuming. Maybe the voice-memo making is the easiest way, but then we need to unify the types or numbers of voice-memos.

We should measure physiological aspects of the users of the human-electric hybrids therefore we can measure how much physical exercise means reaching or keeping an exact speed.

Participants were logistics engineer students. Recording of the routes and times can be a project work for them. Then students get direct feedback from the practical results of their work.

REFERENCES

Straßenverkehrsgesetz (StVG) § 1 Zulassung

https://www.gov.uk/electric-bike-rules (downloaded: 11.01.2018)

1/1975. (II. 5.) KPM-BM együttes rendelet a közúti közlekedés szabályairól

Pneumatic modelling of a pneumobil

Tamás Szakács

University of Óbuda, BGK MEI

1081 Budapest Népszínház u. 8.

+3616665406 szakacs.tamas@bgk.uni-obuda.hu

Abstract: The paper introduces a pneumatic model of a pneumobil vehicle developed at the University of Óbuda. The Matlab/Simulink® model begins at the energy content of the gas stored in the high pressure nitrogen tank, and goes through the thermodynamic, fluid mechanic, and mechanical description of the pressure reducing valve, the pressure, flow, and gas state variables change behavior in the system, the cooperation of the puffer tank, and the pneumatic piston. The goal of the modelling is to describe the air pressure and flow, force, and speed behavior of the piston, in order to optimize drive power, and gas consumption. Further goal of the modelling is to develop, and optimize control strategies, in special attention on maximizing vehicle power, and traveling range.

1. INTRODUCTION

Optimization of a pneumatic propelled vehicle requires a proper description of the pneumatic system.

Modelling the gas behavior in a complex system is not an easy task. The temperature, pressure, the gas flow is continuously changing in time, and space, virtually the gas constant can only be considered constant. There is one quantity that can be considered as base for the description of the thermodynamic and fluid flow, and that is the mass flow.

As the first step I have described the thermodynamic behavior of the gas bottle. The bottle is a constant volume, changing mass system. The enclosed gas amount builds up a pressure, which is changing as the consumption reduces the mass.

The next component is the pressure regulator valve, which is a lot more complex system as the bottle. First of all the mass flow is bidirectional, while the bottle supplies, the consumers consuming the air.

The pneumatic piston is even more complex task, while there is not only pressure building up at a given volume, but the volume is changing as the piston starts moving, and there is also energy transformation from pneumatic to mechanic.

The model was built in Matlab/Simulink® environment. The name of the blocks, functions are their mathematical equations, which helps to understand the logic of the submodels (See Fig.1).

2. DESCRIPTIONS

The following chapters the components of the model will be introduced, and in the last chapter the complete model will be shown.

It was always kept in the focus that the model should remain simple and easy to understand.

Physical quantities are given in practical units (liters, Celsius, bar…) which within the model are converted to SI units: (m^3, Kelvin, Pa). Such converters can be found in all models. Like the one shown in Fig. 1 (l2m^3, C2K Pa2bar)

2.1. The compressed nitrogen bottle model.

As fuel of the pneumobil industrial compressed nitrogen gas is used, which is stored in 10 and 14 liters bottle under 200, and 150 bar pressure. In this model the 10l 200bar bottle is used.

The compressed nitrogen bottle is a constant volume, changing mass thermodynamic system.

The operation of the model: the filled bottle of V volume contains m kg amount of gas which is characterized by R gas constant.

The pressure in the tank can be calculated as:

$$p = \frac{mRT}{V} \qquad (1)$$

The temperature in the tank is considered constant, and equal to the environmental temperature. The consumption of the gas is calculated in the pressure reducing valve submodel.

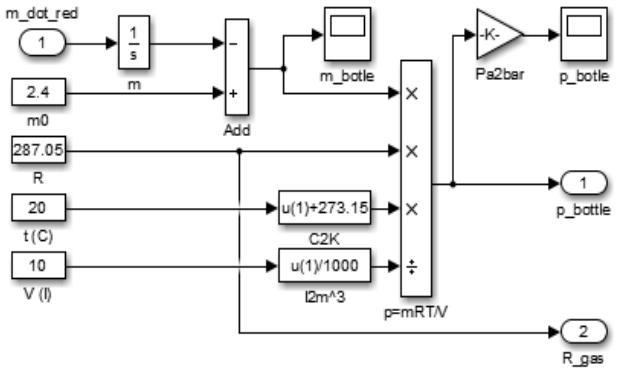

Fig. 1. The pneumatic engine *and its frame.*

If the m_0 initial mass is 2.4 *kg*, the gas constant R=287.05 *J/(kgK)*, bottle volume V=10*l*, temperature t=20^oC, then according to equation (1) the output pressure in the tank is p=202*bar*. This means 201*bar* relative pressure, which is a good approximation of the factory filled industrial nitrogen gas bottle pressure. (200 bar) (Fig. 1). Input is comsumpted mass flow. Output is bottle pressure.

2.2. Pressure regulator model.

The industrial nitrogen gas bottle is coupled to the vehicle by an industrial pressure regulator valve. Fig. 2 shows a pressure regulator cross-section, Fig. 2 shows the internal components.

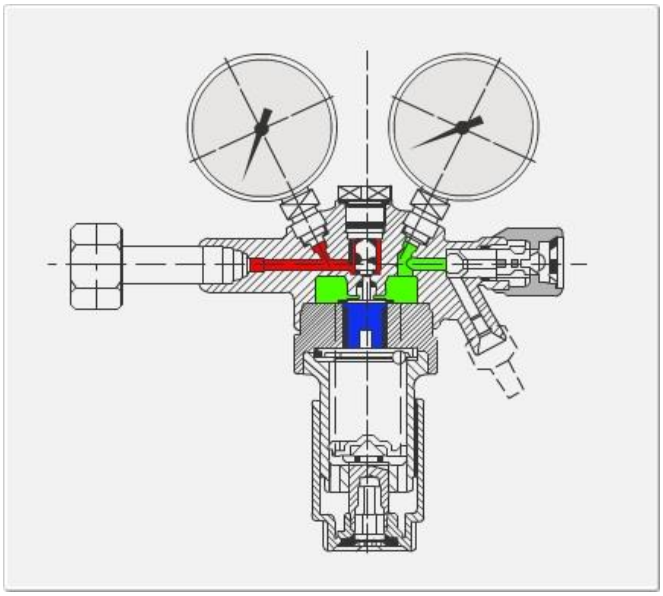

Fig. 2.The construction of the pressure regulator valve [1]

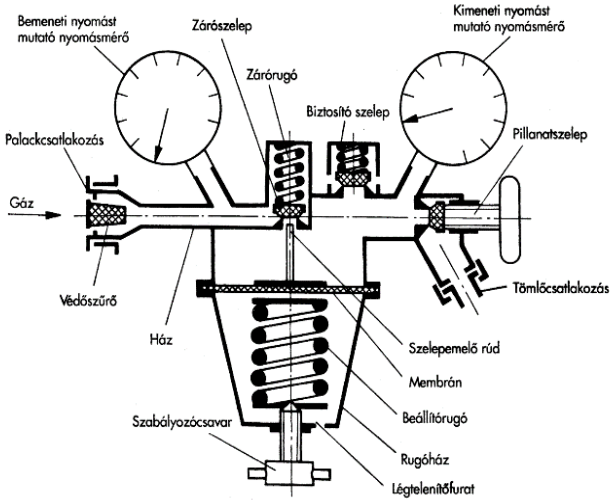

Fig. 3.The components of the pressure regulator valve [2]

The model has the following tasks to fulfill

- to determine the MACH number corresponding to the gas state;
- to determine the reduced pressure gas temperature in the working chamber;
- to calculate the pressure in the regulator working chamber;
- to model the valve closing in the regulator;
- to calculate the gas flow speed, volume, and mass flow.

2.2.1. Calculating gas out speed

Gas flow speed from a pressurized tank is calculated as [3]:

$$v = \sqrt{\frac{2\cdot\kappa}{\kappa-1} R T_t \left[1 - \left(\frac{p_r}{p_t}\right)^{\frac{\kappa-1}{\kappa}}\right]} \left(\frac{m}{s}\right) \quad . \tag{2}$$

2.2.2. Determination of sound speed

The gas exit speed from a tank through a hole without nozzle can not exceed sound, is calculated form adiabatic index, gas constant, and temperature as follows:

$$v_{sound} = \sqrt{\kappa R T} \tag{3}$$

$$M = \frac{v}{v_{sound}} \tag{4}$$

Inputs: Temperature of the reduced pressure gas, gas constant, gas speed.

Output: gas speed limited to 1 MACH

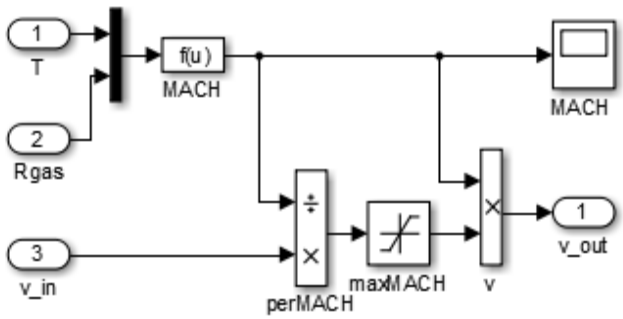

Fig. 4.The 1 MACH limiter

2.2.3. The gas chamber of the pressure regulating valve

The building up of the gas pressure in the regulator chamber is similarly calculated as the pressure is calculated in the high pressure bottle.

The thermodynamic system is a constant volume, variable mass system. The initial mass of the empty chamber builds up an environmental pressure. This can be considered as initial condition.

The integration of the filling/emptying mass flow gives the mass change in the chamber. The equation (1) determines the pressure corresponding the mass of the gas, and the volume of the chamber.

Outputs: absolute value of the chamber pressure.

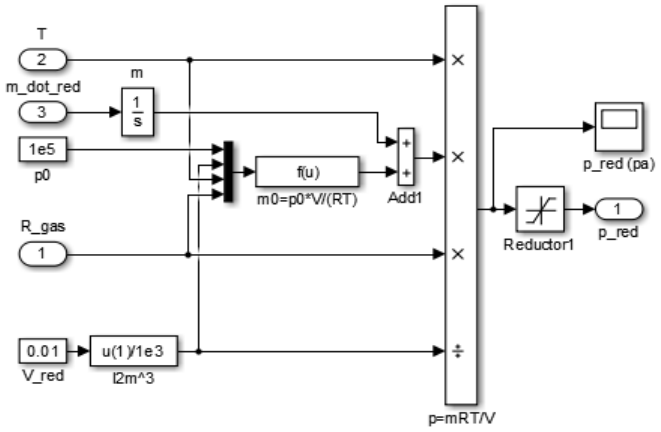

Fig. 5.The gas operating chamber model

2.2.4. The valve model

The task of the valve is to close the way of the mass flow, when the se pressure is achieved. When gas is consumed from the operating chamber, the valve opens, and closes again, when the pressure has built up again. Opening, and closing the valve is described by adjusting the cross section (d diameter, and h gap) of the valve.

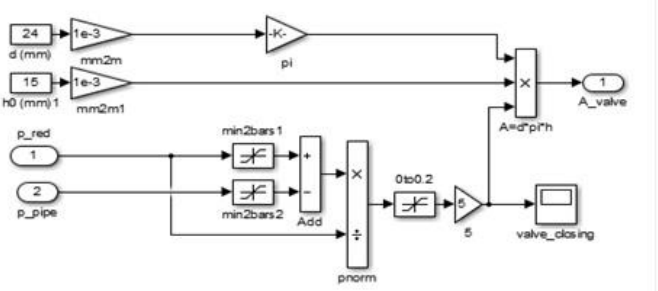

Fig. 6. The valve model

Besides the two submodels, the following calculation are done in the pressure regulator valve model

A block, called regulator, reduces the bottle pressure to the set value, which is in this case 10 bars.

The temperature of the reduced pressure gas can be calculated as adiabatic gas state change as follows:

The gas speed in the pressure regulator is calculated in equation 2:

Δp is the difference between bottle, and reduced pressure

The average density:

$$\varrho = \frac{\Delta p}{RT} \quad \left(\frac{kg}{m^3}\right) \qquad (5)$$

The volume flow:

$$\dot{V} = Av \quad \left(\frac{m^3}{s}\right) \qquad (6)$$

where A is the cross section of the valve. The mass flow:

$$\dot{m} = \varrho V \quad \left(\frac{\dot{kg}}{s}\right) \qquad (7)$$

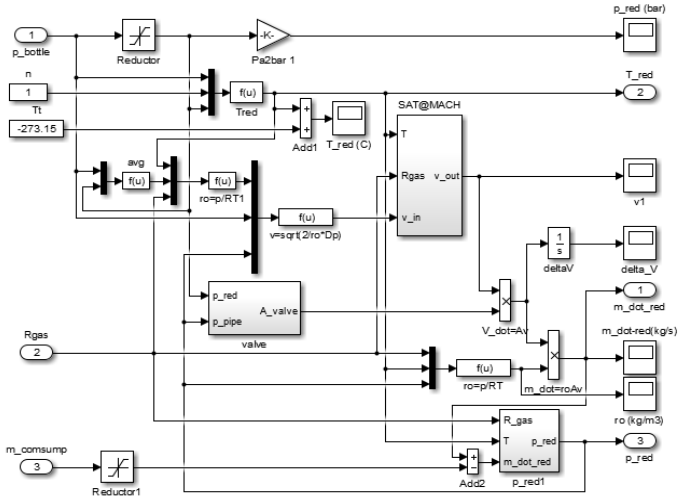

Fig. 7. Pressure regulator model

2.3. The puffer tank model

Operation of the model:
The tank of V volume at initial state contains m_0 gas, which builds up p_0 pressure, which is in balance with the ambient pressure.

$$m_0 = \frac{p_0 V}{RT}\ (kg)\ . \qquad (8)$$

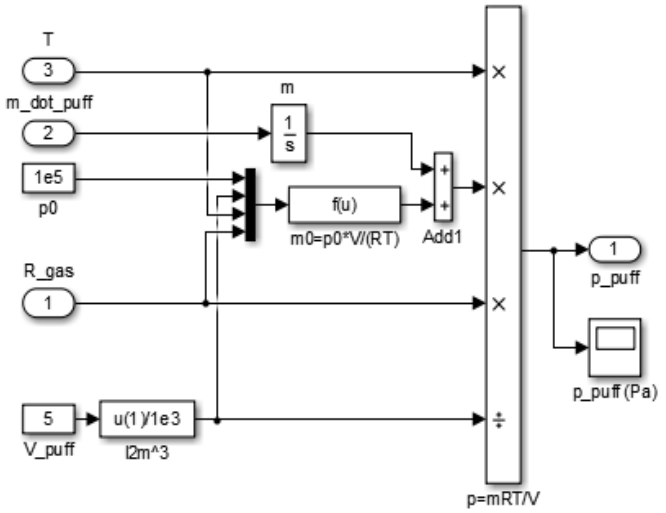

Fig. 8. Puffer tank model

The integration of the filling/emptying mass flow gives the mass change in the puffer tank. The equation (1) determines the pressure corresponding the mass of the gas, and the volume of the puffer.

Model inputs: 1: R_{gas}:gas constant, 2 mass flow, 3 temperature.

Variables: $p_0=10^5 Pa$

$V_{puff}= 5l$

2.4. Pneumatic cylinder model

The pneumatic work cylinder thermodynamically is similar to the puffer tank. The main difference is that, the volume of the cylinder changes as soon the piston starts moving.

The enclosed gas amount in cylinder volume is calculated similarly to the initial mass in the puffer tank. This amount is reset each time when a cylinder is reversed.

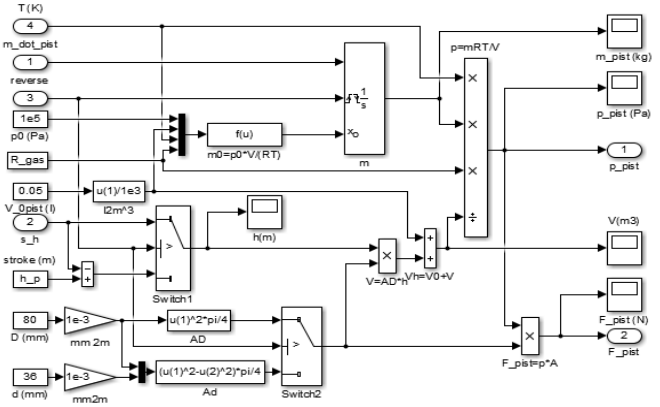

Fig. 9. Pneumatic cylinder model

This version of model has only one chamber (switched chamber modelling). Cylinder reset is modelled by releasing current pressure, and resetting the initial gas amount in the chamber. Reversed cylinder has different piston cross section area, while on the reverse side the cross section is decreased by the piston rod. A_D is the outer, A_d is the inner motion piston cross section respectively.

The two switches in the model are to switch data in the out-, and the instroke motion, and by calculating in and out distances.

2.5. Vehicle body model

The vehicle body model is a simplified mechanical inertia model. It calculates acceleration from the acting force, and by double integration determines traveling speed, and distance. Fix, and variable gears are taken into consideration, as well as wind resistance. Because of the piston motion is mechanically linked to vehicle motion, the former is also in this model determined, as well as piston end position signals are determined here for reversing the stroke.

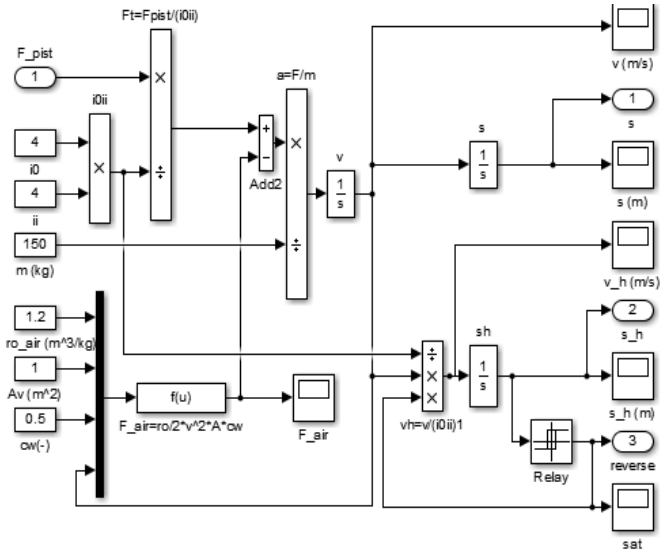

Fig. 10. Puffer tank model

2.6. *The full pneumatic model*

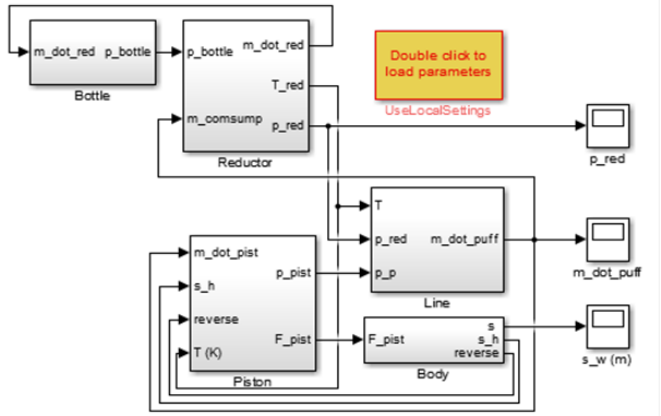

Fig. 11. The full model

The upper layer of the Simulink model connects the individual submodels. The model can be extended by further components, like double chamber piston model, puffer tank, driver or controller model.

3. MODELLING

At this state of the model many different aspects can be investigated. For example effect of regulator set pressure, the piston diameter, stroke, transmission gear modification ratio effect of the air resistance, on maximum speed, or travelled distance.

Every detail of gas state variable change, pressure, force speed, and distance data can be looked after, optimizations can be run.

4. RESULTS

In the following set of pictures some simulation data will be provided.

For the test run, in case of simplicity a very fast run is presented, in order to be able showing the results in short diagrams. In each diagram timescale is in seconds

Fig. 12 shows the speed of the car as a function of time.

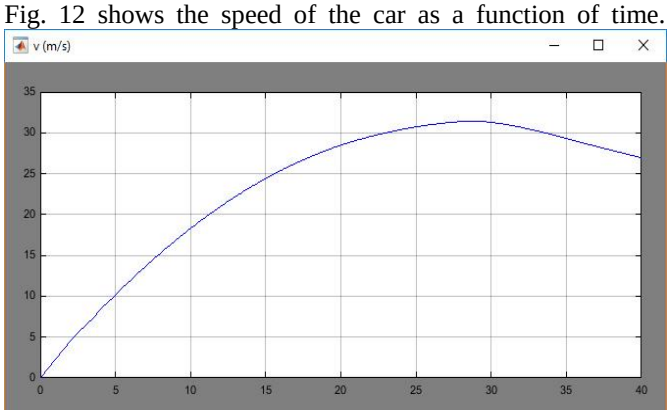

Fig. 12. Speed of the car

The corresponding piston pressures during the run:

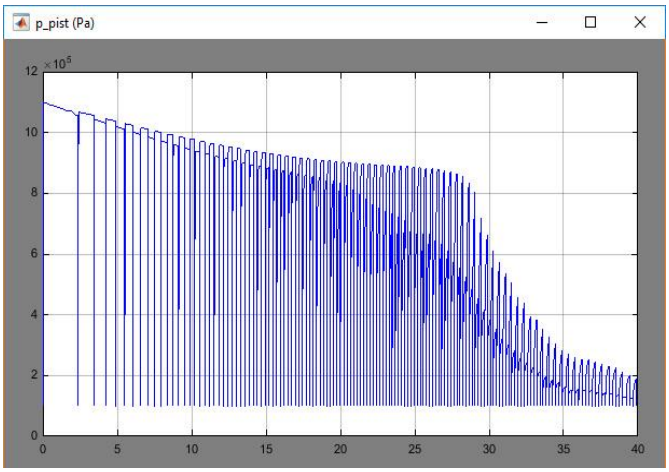

Fig. 13. Piston pressure during the run

It can be seen that the piston is asymmetric. One side has bigger cross section, the opposite side, where the piston rod is located has smaller. the vehicle starts by using the bigger cross section side, and after the end position switches to reverse direction. The pressure is building up in a different way, that can be seen in the figure.

Piston forces are fluctuating similarly to the pressure. it can be seen that the bigger cross section produces greater piston force. Fig. 14 shows the forces at the entire run, 15 the first 7 seconds, and Fig. 16 shows the building up the force at the beginning of the stroke.

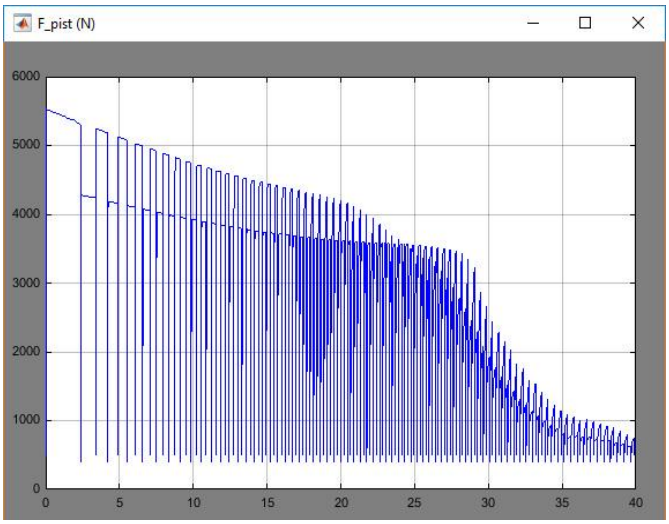

Fig. 14. Piston forces during the run

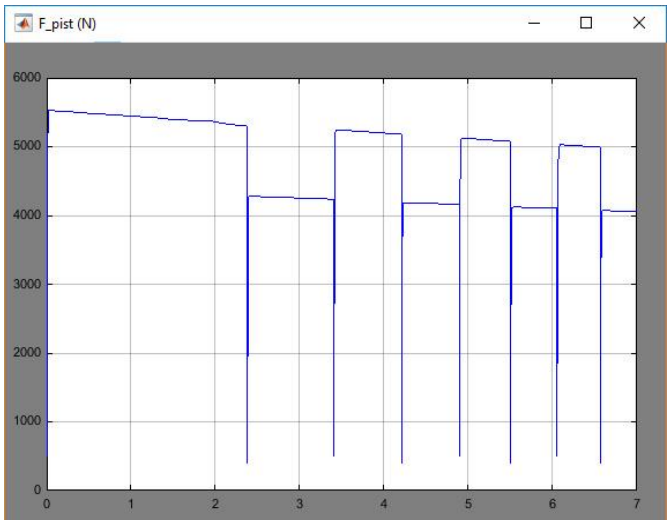

Fig. 15. Piston forces during the run zoomed

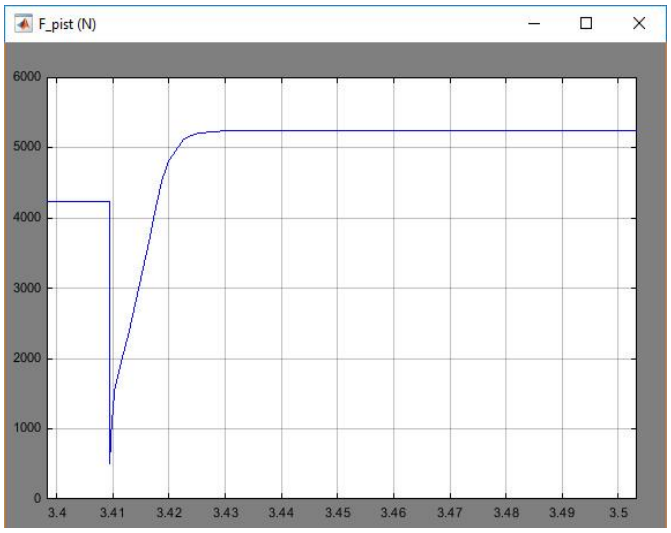

Fig. 16. Piston force building up

Fig. 17 shows the speed of the cylinder during the entire run.

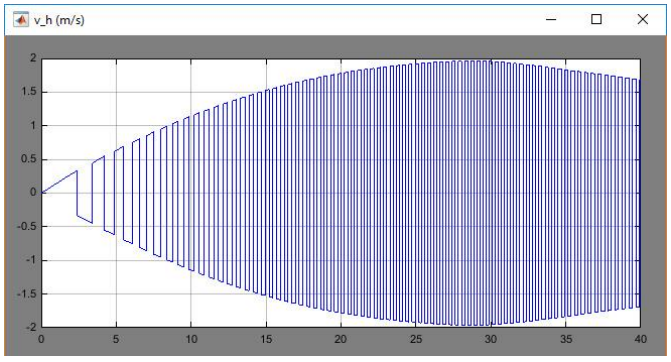

Fig. 17. Piston speed during the run.

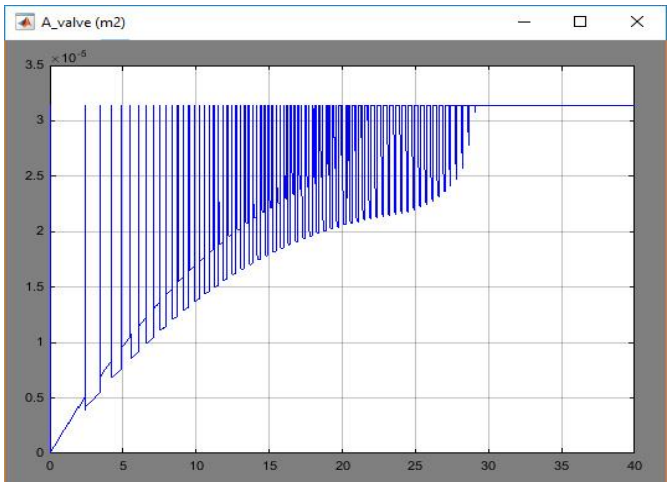

Fig. 18. Pressure regulator valve cross section

Fig. 18 shows the pressure regulator valve cross section during the run

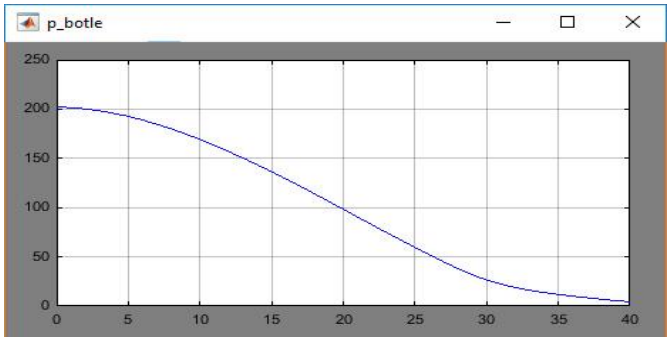

Fig. 19. Bottle pressure during the run

5. CONCLUSIONS, RECOMMENDATIONS

The model is being validated by measuring results, which is not introduced in this paper. The further development of the model is including double chamber piston (instead of the recent switched chamber), and controller logic, in order to develop economic drive control.

REFERENCES

[1] http://www.tankonyvtar.hu/hu/tartalom/tamop412A/2010-0017_22_ipari_gazok/ch02s03.html
[2] http://tudasbazis.sulinet.hu/hu/szakkepzes/gepeszet/gepeszeti-szakismeretek-1/langhegesztes-alkalmazasa-anyagai-eszkozei/langhegeszto-berendezesek-reszegysegei
[3] Kulmann László Áramlástechnika Typotex kiadó, 2012 ISBN 978-963-279-533-1